Cell Reports Medicine, Volume *5*

Supplemental information

A vaccine targeting antigen-presenting cells through CD40 induces protective immunity against Nipah disease

Yadira Pastor, Olivier Reynard, Mathieu Iampietro, Mathieu Surenaud, Florence Picard, Nora El Jahrani, Cécile Lefebvre, Adele Hammoudi, Léa Dupaty, Élise Brisebard, Stéphanie Reynard, Élodie Moureaux, Marie Moroso, Stéphanie Durand, Claudia Gonzalez, Lucia Amurri, Anne-Sophie Gallouët, Romain Marlin, Sylvain Baize, Eve Chevillard, Hervé Raoul, Hakim Hocini, Mireille Centlivre, Rodolphe Thiébaut, Branka Horvat, Véronique Godot, Yves Lévy, and Sylvain Cardinaud

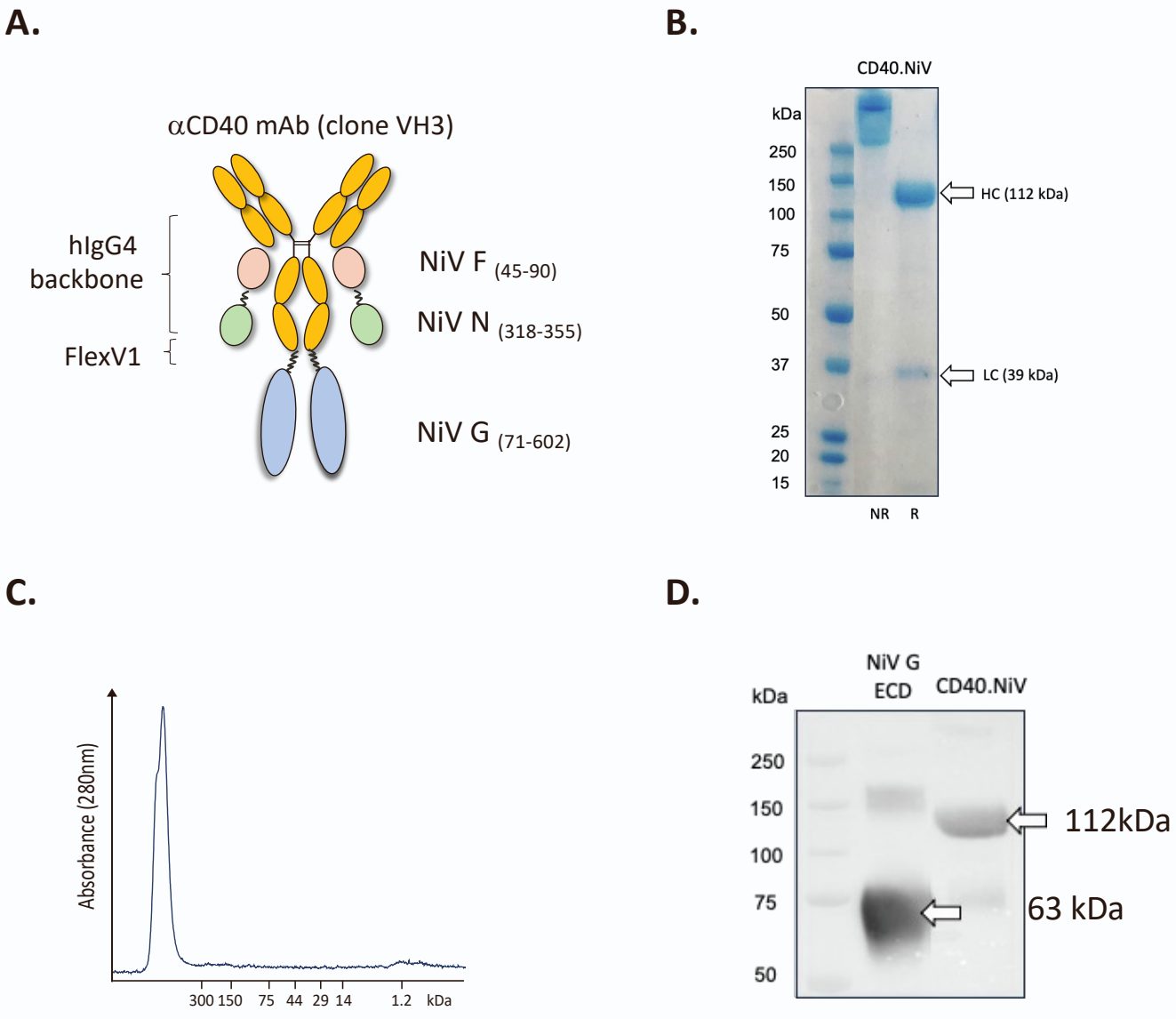

Figure S1. Structure and quality control of the CD40.NiV vaccines. Related to Figure 1. **(A)** Schematic representation of CD40.NiV. **(B)** SDS-PAGE profiles of non-reduced (NR) versus reduced (R) conditions. Molecular weight (kDa) markers are shown on the left. Arrows indicate the heavy chain (HC) and light chain (LC) of the vaccine. Sizes were predicted based on the amino acid composition. Given the glycosylated state of NiV G, bands are presented as predicted. **(C)** Size exclusion chromatography (SEC 10/300) of the vaccine (blue line). Standard protein molecular weight markers are indicated. The unique pic corresponding to the recombinant mAbs is indicated by the arrows. **(D)** Fusion of the NiV-B G ECD to the CD40.NiV vaccine was confirmed by western-blotting using sera from NiV-B G-immunized mice and testing the in-house produced NiV G ECD as a positive control (right).

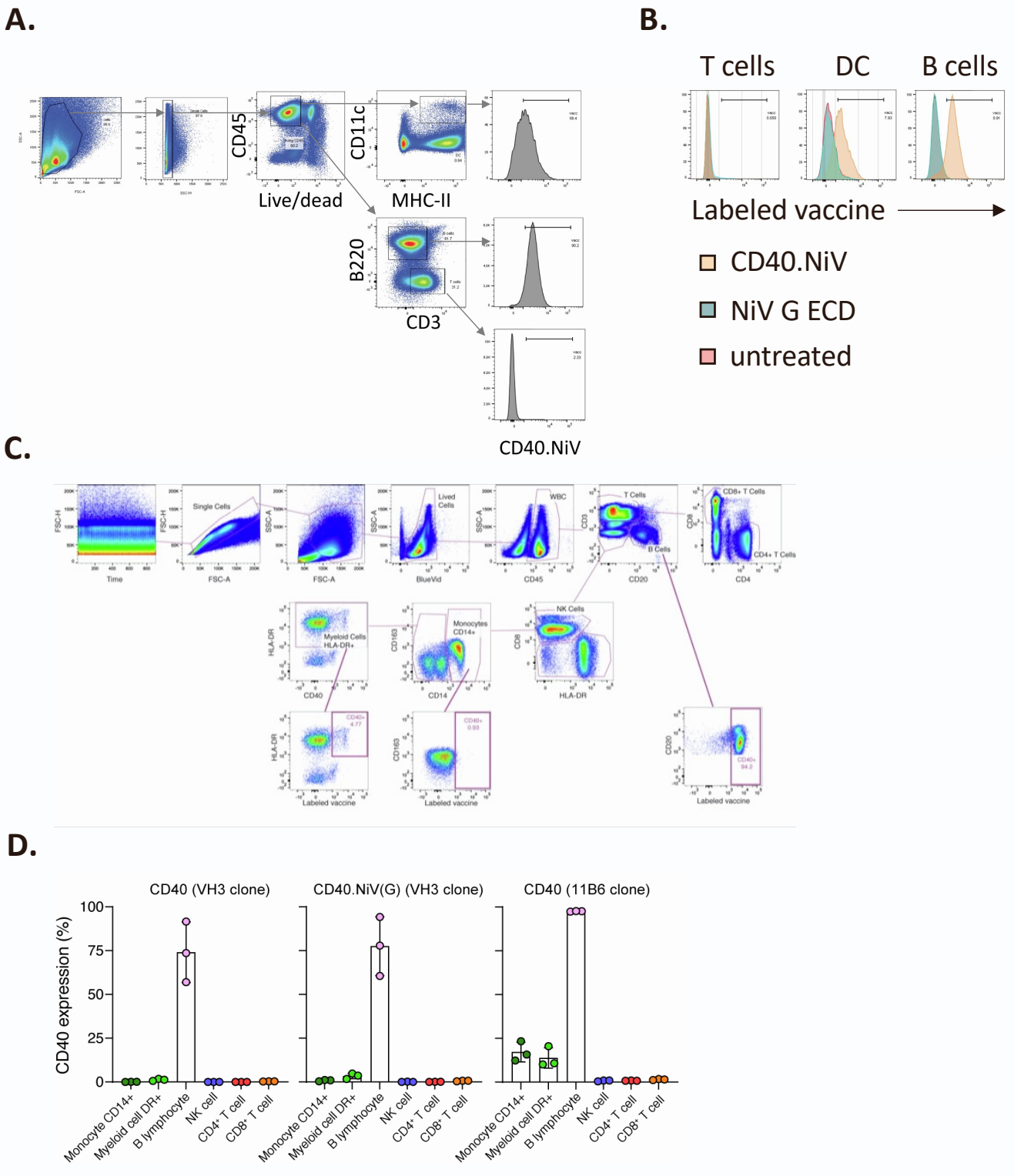

Figure S2. CD40.NiV binds the human CD40 receptor. Related to Figure 1. Splenocytes of hCD40Tg mice were incubated with 1 nM APC-labeled CD40.NiV (brown), non-targeting NiV G ECD (green), or untreated (salmon) and subsequently labeled for T-, B- and DC cell markers. **(A)** Gating strategy. T-cells were gated on $CD45^{+}$ $CD3^{+}$ cells, DC on $CD11c^{+}$, $MHC\text{-}II^{hi}$ and B-cells on $CD45^{+}$ $B220^{+}$. **(B)** Histogram (MFI) of labeled vaccines on each gated population. Graphs are representative of 2 experiments. **(C)** Same as A, using PBMCs from naïve African green monkeys (AGM) (n=3). Gating strategy. $CD8^{+}$ and $CD4^{+}$ T-cells were gated on $CD3^{+}$ cells, while B-cells were $CD20^{+}$. Among $CD3^{neg}$, NK cells were $HLA\text{-}DR^{neg}$ $CD8^{+}$, while myeloid cells were distinguished from monocytes by HLA-DR and CD14 expression, respectively. **(D)** The original anti-CD40 clone (12E12/VH3) and another in-house-derived clone (11B6) [53] with no associated antigens were used as positive controls. Binding of the vaccine was demonstrated on B-cells, which express CD40, and to a lesser extent on monocyte/ myeloid DR^{+} populations.

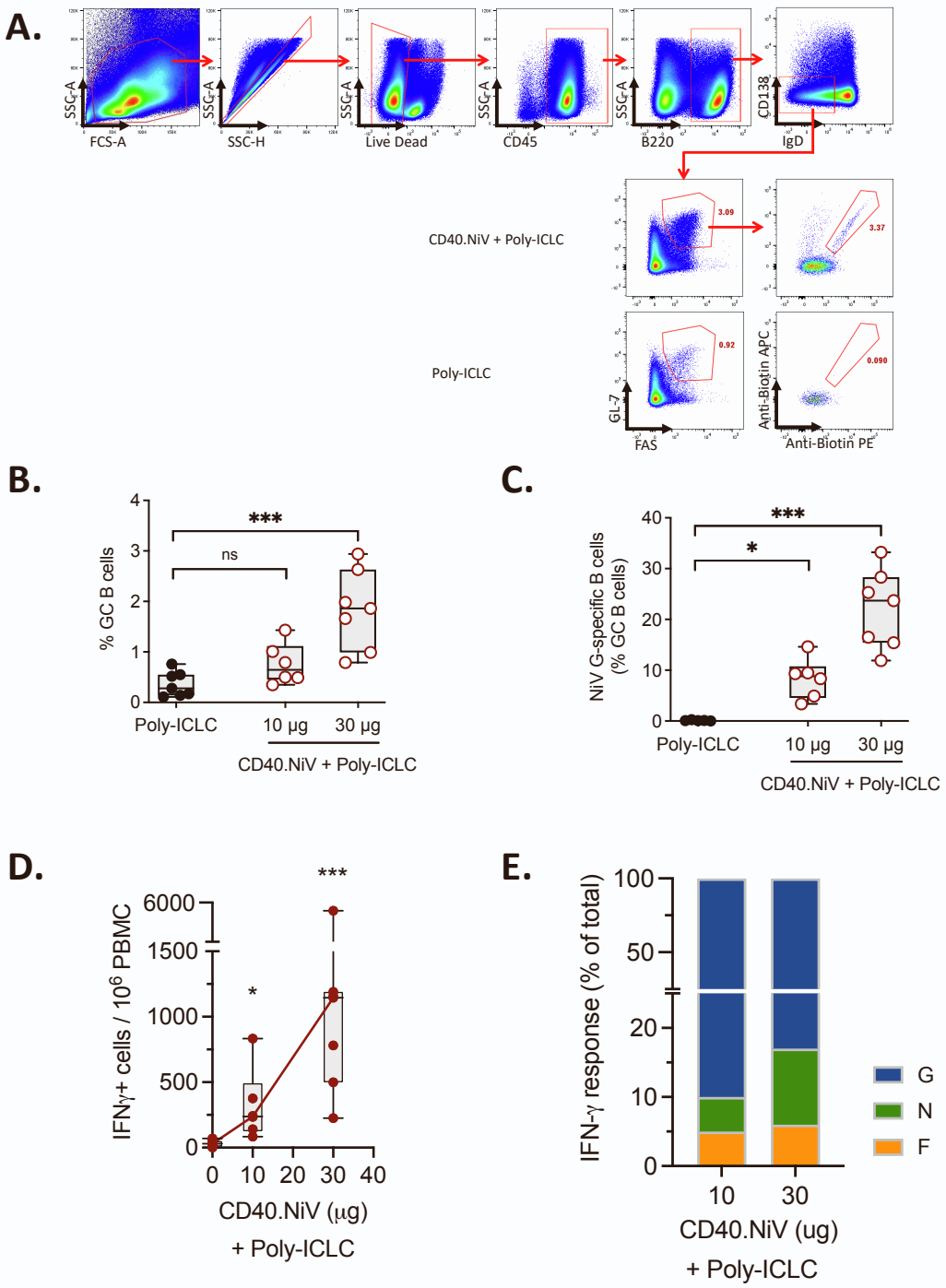

Figure S3. Mouse NiV G-specific B- and T-cells responses in draining lymph nodes. Related to Figure 2. (A) Mouse NiV G-specific B-cells were stained using biotinylated NiV G protein. Gating strategy. FAS^+ $GL\text{-}7^+$ germinal center (GC) B-cells were gated on $B220^+$, IgD^- $CD138^-$ cells, and NiV G-specific GC B-cells considered to be double positive for the anti-biotin staining. Representative dot plots of mice immunized with 10 µg of CD40.NiV (+Poly-ICLC) or with adjuvant alone are represented. **(B)** Percentage (%) of GC B-cells and **(C)** NiV G-specific B-cells among GC B-cells, in mice immunized with CD40.NiV (10 versus 30 µg, with Poly-ICLC) or Poly-ICLC alone. Non-parametric Kruskal-Wallis tests with Dunn's multiple comparison post-hoc test; $*P < 0.05$, $***P < 0.001$. **(D)** Dose dependent polyepitopic T-cells responses to CD40.NiV in hCD40Tg mice. As in Figure 2, IFN-γ T-cell responses to the NiV G, F, and N overlapping peptide pools assessed from spleens by ELISpot one week post-boost. Animals were immunized with 10 µg versus 30 µg of CD40.NiV with poly-ICLC and the responses compared to those of the poly-ICLC only negative group. The total number of spots are reported per million splenocytes (background subtracted). Non-parametric Kruskal-Wallis tests with Dunn's multiple comparison post-hoc test; *P < 0.05, ***P < 0.001. **(E)** Percentage of NiV G (blue), N (green), and F (orange) peptide-specific IFN-γ responses for 10 and 30 µg of vaccine. Data are representative of at least two experiments.

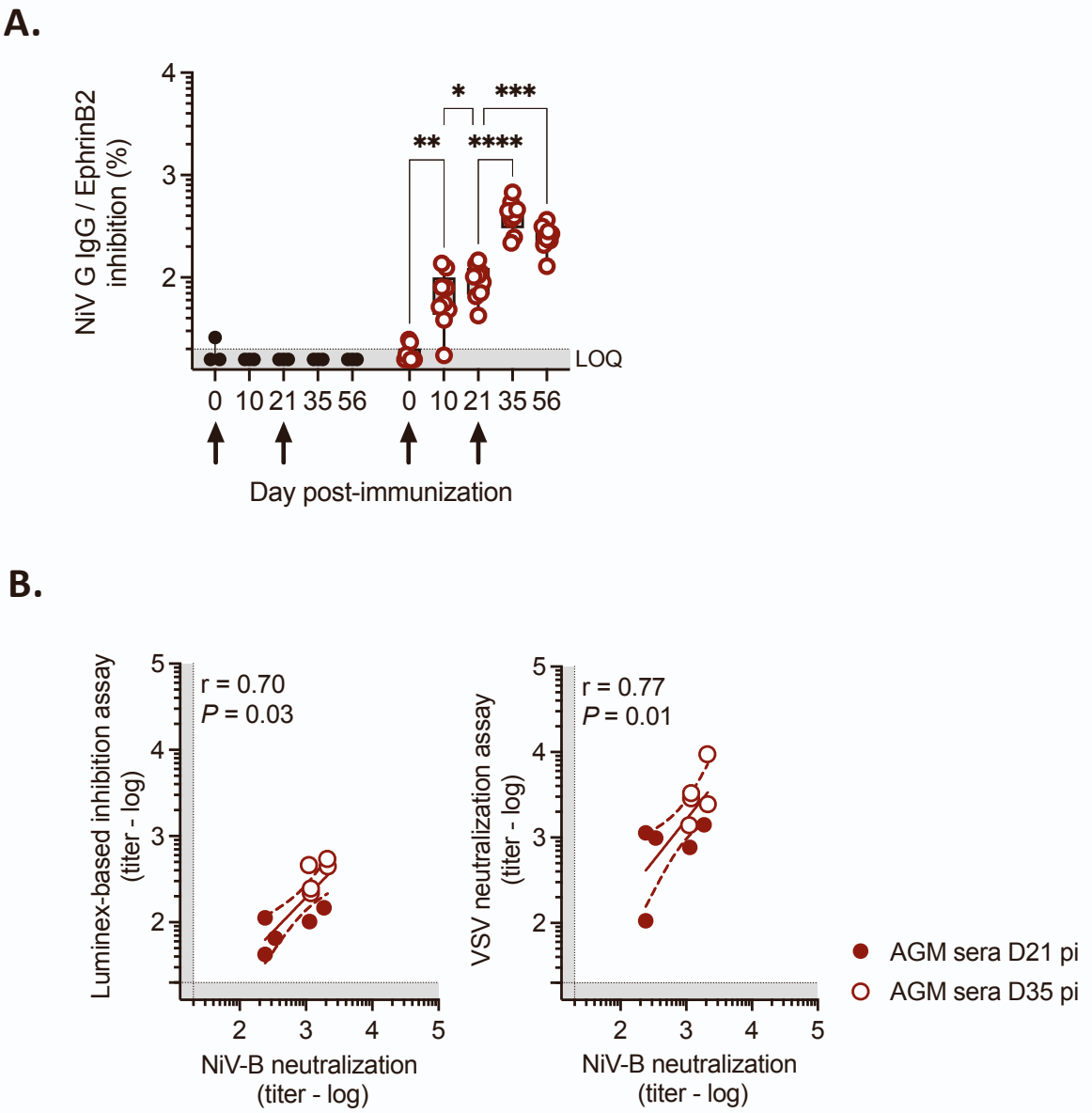

Figure S4. Serum neutralization assay in AGMs Related to Figure 3. **(A)** As in Figure 3, neutralization of AGM sera was confirmed using a Luminex-based inhibition assay on sequential time points. Non-parametric Kruskal-Wallis tests with Dunn's multiple comparison post-hoc test; *$P < 0.05$, ** $P < 0.01$, *** $P < 0.001$, **** $P < 0.0001$. **(B)** Neutralization titers evaluated in sera from CD40.NiV AGMs collected on days 21 and 35 post-immunization were correlated to titers evaluated by the Luminex-based inhibition assay (left) and the VSV (F/G) infection model (right).

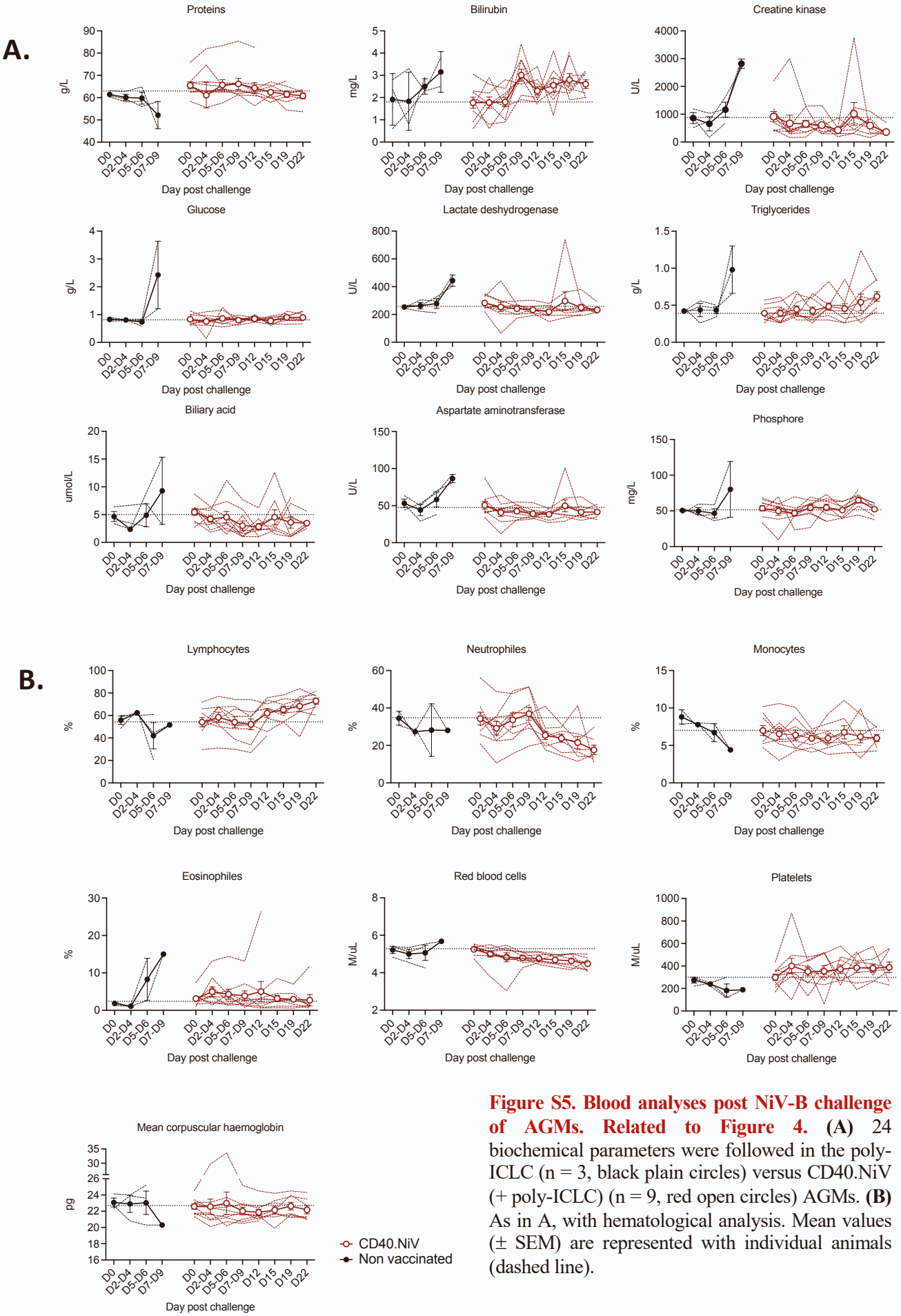

Figure S5. Blood analyses post NiV-B challenge of AGMs. Related to Figure 4. **(A)** 24 biochemical parameters were followed in the poly-ICLC (n = 3, black plain circles) versus CD40.NiV (+ poly-ICLC) (n = 9, red open circles) AGMs. **(B)** As in A, with hematological analysis. Mean values (± SEM) are represented with individual animals (dashed line).

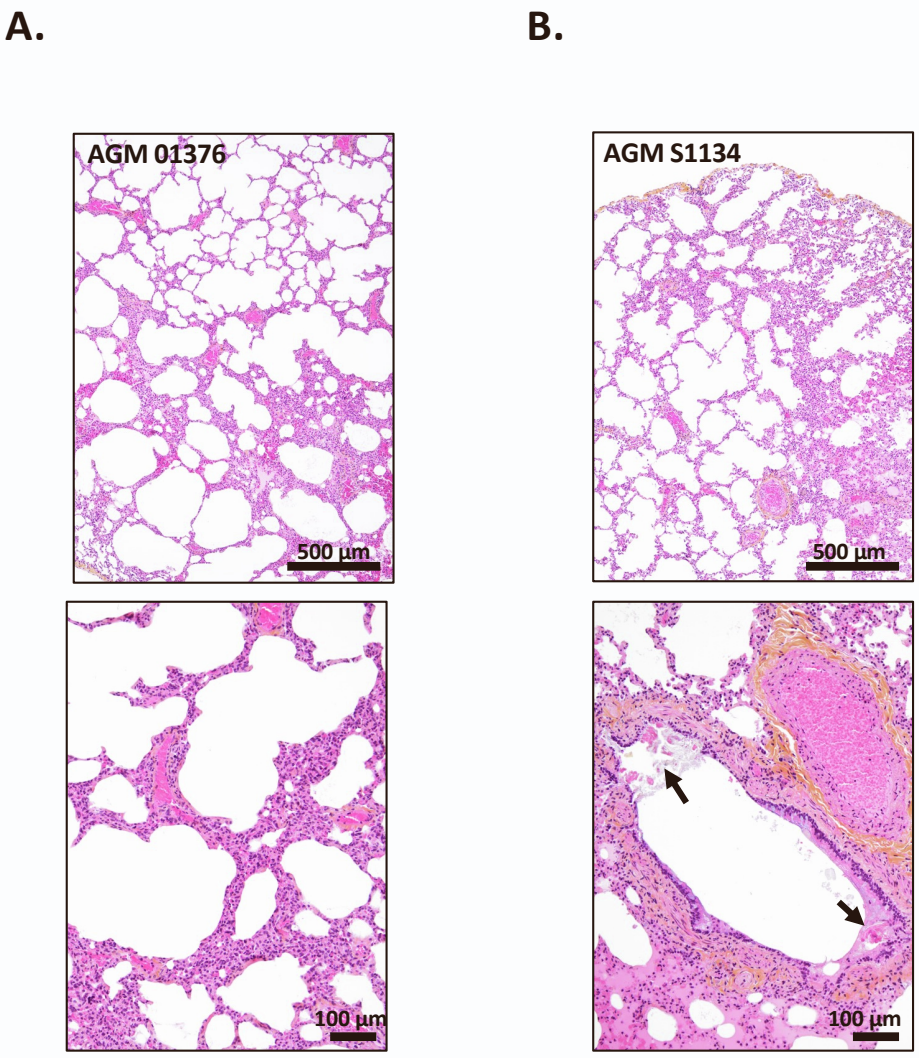

Figure S6. Illustration of mild histopathological changes observed in the lungs of two vaccinated animals. Related to Figure 4. Hematoxylin-eosin staining showed **(A)** traces of interstitial pneumonia (thickening of the alveolar septa by inflammatory cell infiltration, without syncytial formation) in AGM #O1376 and **(B)** traces of mucus in the bronchia (arrows) in AGM #S1134.

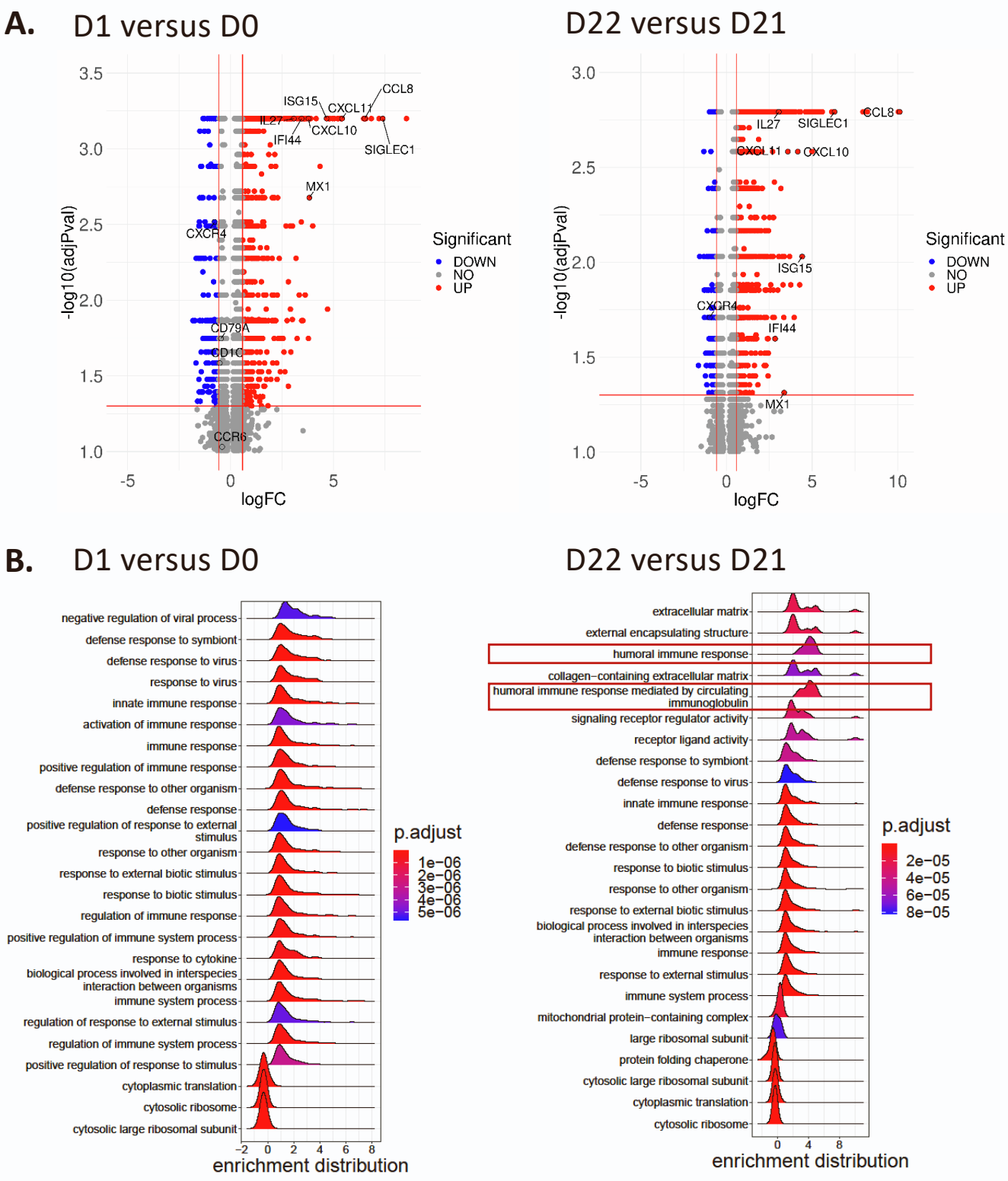

Figure S7. Characterization of gene expression profiles post prime (D1 versus D0) and post boost (D22 versus D21). Related to Figure 7. **(A)** Volcano plots of DEGs between D1 and D0 (left) and D22 and D21 (right). Down- and upregulated genes are shown in blue and red, respectively. The top 35 most upregulated and downregulated genes based on the log2FC are depicted. **(B)** Gene set enrichment analysis was performed on differentially expressed genes with an adjusted p-value ≤ 0.05 between D1 and D0 (left) and D22 and D21 (right) using the ClusterProfiler v4.4.4 R package. The density plot shows the top 25 pathways based on the adjusted p-value and normalized enrichment score.

Table S1: The amino acid sequences of the vaccine antigens and the mutations present between the tested strains of NiV-B, M, C, and HeV. **Related to Figure 1.**

NiV G $_{71\text{-}602}$

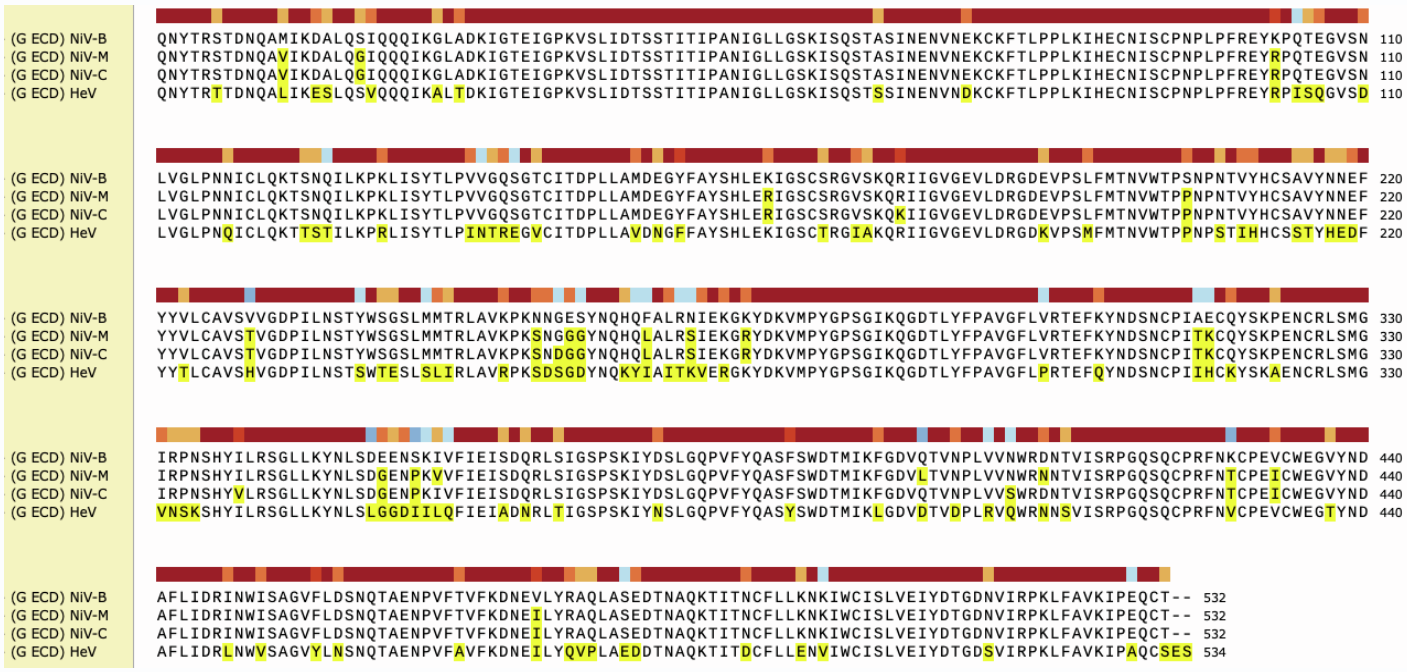

NiV F $_{45\text{-}90}$

NiV N $_{318\text{-}355}$

Table S2: Pools of overlapping peptides. **Related to Figure 2**

NiV G ECD

Peptide #	Position	AA sequence	Peptide #	Position	AA sequence	Peptide #	Position	AA sequence
1	61	VIIVMNIMIIQNYTR	44	233	HLERIGSCSRGVSKQ	89	413	LLKYNLSDGENPKVV
2	65	MNIMIIQNYTRSTDN	45	237	IGSCSRGVSKQRIIG	90	417	NLSDGENPKVVFIEI
3	69	IIQNYTRSTDNQAVI	46	241	SRGVSKQRIIGVGEV	91	421	GENPKVVFIEISDQR
4	73	YTRSTDNQAVIKDAL	47	245	SKQRIIGVGEVLDRG	92	425	KVVFIEISDQRLSIG
5	77	TDNQAVIKDALQGIQ	48	249	IIGVGEVLDRGDEVP	93	429	IEISDQRLSIGSPSK
6	81	AVIKDALQGIQQQIK	49	253	GEVLDRGDEVPSLFM	94	433	DQRLSIGSPSKIYDS
7	85	DALQGIQQQIKGLAD	50	257	DRGDEVPSLFMTNVW	95	437	SIGSPSKIYDSLGQP
8	89	GIQQQIKGLADKIGT	51	261	EVPSLFMTNVWTPPN	96	441	PSKIYDSLGQPVFYQ
9	93	QIKGLADKIGTEIGP	52	265	LFMTNVWTPPNPNTV	97	445	YDSLGQPVFYQASFS
10	97	LADKIGTEIGPKVSL	53	269	NVWTPPNPNTVYHCS	98	449	GQPVFYQASFSWDTM
11	101	IGTEIGPKVSLIDTS	54	273	PPNPNTVYHCSAVYN	99	453	FYQASFSWDTMIKFG
12	105	IGPKVSLIDTSSTIT	55	277	NTVYHCSAVYNNEFY	100	457	SFSWDTMIKFGDVLT
13	109	VSLIDTSSTITIPAN	56	281	HCSAVYNNEFYYVLC	101	461	DTMIKFGDVLTVNPL
14	113	DTSSTITIPANIGLL	57	285	VYNNEFYYVLCAVST	102	465	KFGDVLTVNPLVVNW
15	117	TITIPANIGLLGSKI	58	289	EFYYVLCAVSTVGDP	103	469	VLTVNPLVVNWRNNT
16	121	PANIGLLGSKISQST	59	293	VLCAVSTVGDPILNS	104	473	NPLVVNWRNNTVISR
17	125	GLLGSKISQSTASIN	60	297	VSTVGDPILNSTYWS	105	477	VNWRNNTVISRPGQS
18	129	SKISQSTASINENVN	61	301	GDPILNSTYWSGSLM	106	481	NNTVISRPGQSQCPR
19	133	QSTASINENVNEKCK	62	305	LNSTYWSGSLMMTRL	107	485	ISRPGQSQCPRFNTC
20	137	SINENVNEKCKFTLP	63	309	YWSGSLMMTRLAVKP	108	489	GQSQCPRFNTCPEIC
21	141	NVNEKCKFTLPPLKI	64	313	SLMMTRLAVKPKSNG	109	493	CPRFNTCPEICWEGV
22	145	KCKFTLPPLKIHECN	65	317	TRLAVKPKSNGGGYN	110	497	NTCPEICWEGVYNDA
23	149	TLPPLKIHECNISCP	66	321	VKPKSNGGGYNQHQL	111	501	EICWEGVYNDAFLID
24	153	LKIHECNISCPNPLP	67	325	SNGGGYNQHQLALRS	112	505	EGVYNDAFLIDRINW
25	157	ECNISCPNPLPFREY	68	329	GYNQHQLALRSIEKG	113	509	NDAFLIDRINWISAG
26	161	SCPNPLPFREYRPQT	69	333	HQLALRSIEKGRYDK	114	513	LIDRINWISAGVFLD
27	165	PLPFREYRPQTEGVS	70	337	LRSIEKGRYDKVMPY	115	517	INWISAGVFLDSNQT
28	169	REYRPQTEGVSNLVG	71	341	EKGRYDKVMPYGPSG	116	521	SAGVFLDSNQTAENP
29	173	PQTEGVSNLVGLPNN	72	345	YDKVMPYGPSGIKQG	117	525	FLDSNQTAENPVFTV
30	177	GVSNLVGLPNNICLQ	73	349	MPYGPSGIKQGDTLY	118	529	NQTAENPVFTVFKDN
31	181	LVGLPNNICLQKTSN	74	353	PSGIKQGDTLYFPAV	119	533	ENPVFTVFKDNEILY
32	185	PNNICLQKTSNQILK	75	357	KQGDTLYFPAVGFLV	120	537	FTVFKDNEILYRAQL
33	189	CLQKTSNQILKPKLI	76	361	TLYFPAVGFLVRTEF	121	541	KDNEILYRAQLASED
34	193	TSNQILKPKLISYTL	77	365	PAVGFLVRTEFKYND	122	545	ILYRAQLASEDTNAQ
35	197	ILKPKLISYTLPVVG	78	369	FLVRTEFKYNDSNCP	123	549	AQLASEDTNAQKTIT
36	201	KLISYTLPVVGQSGT	79	373	TEFKYNDSNCPITKC	124	553	SEDTNAQKTITNCFL
37	205	YTLPVVGQSGTCITD	80	377	YNDSNCPITKCQYSK	125	557	NAQKTITNCFLLKNK
38	209	VVGQSGTCITDPLLA	81	381	NCPITKCQYSKPENC	126	561	TITNCFLLKNKIWCI
39	213	SGTCITDPLLAMDEG	82	385	TKCQYSKPENCRLSM	127	565	CFLLKNKIWCISLVE
40	217	ITDPLLAMDEGYFAY	83	389	YSKPENCRLSMGIRP	128	569	KNKIWCISLVEIYDT
41	221	LLAMDEGYFAYSHLE	84	393	ENCRLSMGIRPNSHY	129	573	WCISLVEIYDTGDNV
42	225	DEGYFAYSHLERIGS	85	397	LSMGIRPNSHYILRS	130	577	LVEIYDTGDNVIRPK
43	229	FAYSHLERIGSCSRG	86	401	IRPNSHYILRSGLLK	131	581	YDTGDNVIRPKLFAV
			87	405	SHYILRSGLLKYNLS	132	585	DNVIRPKLFAVKIPE
			88	409	LRSGLLKYNLSDGEN	133	588	IRPKLFAVKIPEQCT

NiV F peptide

Peptide #	Position	AA sequence
1	1	KYKIKSNPLTKDIVI
2	5	KSNPLTKDIVIKMIP
3	9	LTKDIVIKMIPNVSN
4	13	IVIKMIPNVSNMSQC
5	17	MIPNVSNMSQCTGSV
6	21	VSNMSQCTGSVMENY
7	25	SQCTGSVMENYKTRL
8	29	GSVMENYKTRLNGIL
9	33	MENYKTRLNGILTPI

NiV N peptide

Peptide #	Position	AA sequence
1	1	IQTKFAPGGYPLLWS
2	5	FAPGGYPLLWSFAMG
3	9	GYPLLWSFAMGVATT
4	13	LWSFAMGVATTIDRS
5	17	AMGVATTIDRSMGAL
6	21	ATTIDRSMGALNINR
7	24	IDRSMGALNINRGYL